European Journal of Pharmaceutics and Biopharmaceutics 117 (2017) 91–104

Contents lists available at ScienceDirect

European Journal of Pharmaceutics and Biopharmaceutics

journal homepage: www.elsevier.com/locate/ejpb

Micro-Flow Imaging as a quantitative tool to assess size and agglomeration of PLGA microparticles

Miranda M.C. van Beers [a,b], Cees Slooten [a], Jelte Meulenaar [a], Ahmad S. Sediq [b], Ruud Verrijk [a], Wim Jiskoot [b,*]

[a] Dr. Reddy's Research & Development B.V., Zernikedreef 12, 2333 CL Leiden, The Netherlands
[b] Division of Drug Delivery Technology, Cluster BioTherapeutics, Leiden Academic Centre for Drug Research, Leiden University, Leiden, The Netherlands

ARTICLE INFO

Article history:
Received 24 January 2017
Accepted in revised form 5 April 2017
Available online 6 April 2017

Keywords:
Agglomeration
Flow imaging microscopy
Octreotide acetate
Particle size
PLGA microparticles
Risperidone

ABSTRACT

The purpose of this study was to explore the potential of flow imaging microscopy to measure particle size and agglomeration of poly(lactic-co-glycolic acid) (PLGA) microparticles. The particle size distribution of pharmaceutical PLGA microparticle products is routinely determined with laser diffraction. In our study, we performed a unique side-by-side comparison between MFI 5100 (flow imaging microscopy) and Mastersizer 2000 (laser diffraction) for the particle size analysis of two commercial PLGA microparticle products, i.e., Risperdal Consta and Sandostatin LAR. Both techniques gave similar results regarding the number and volume percentage of the main particle population (28–220 µm for Risperdal Consta; 16–124 µm for Sandostatin LAR). MFI additionally detected a 'fines' population (<28 µm for Risperdal Consta; <16 µm for Sandostatin LAR), which was overlooked by Mastersizer. Moreover, MFI was able to split the main population into 'monospheres' and 'agglomerates' based on particle morphology, and count the number of particles in each sub-population. Finally, we presented how MFI can be applied in process development of risperidone PLGA microparticles and to monitor the physical stability of Sandostatin LAR. These case studies showed that MFI provides insight into the effect of different process steps on the number, size and morphology of fines, monospheres and agglomerates as well as the extent of microparticle agglomeration after reconstitution. This can be particularly important for the suspendability, injectability and release kinetics of PLGA microparticles.

1. Introduction

Microencapsulation of drugs that are otherwise rapidly degraded or cleared from the body can prolong the therapeutic effect from days to several weeks or months [1]. Injectable microparticles composed of poly(lactic-co-glycolic acid) (PLGA) polymers are one of the most successful controlled drug delivery systems, which overcome the need of frequent injections and thereby improve patient compliance and comfort [2,3]. Better regulation of the drug release rate also reduces variability in blood levels, which increases the safety and efficacy of the encapsulated drug. PLGA microparticles largely owe their success to the biocompatibility, biodegradability and adjustable release kinetics of PLGA polymers.

Two examples of PLGA microparticle products that were successfully introduced in the clinic are Risperdal Consta and Sandostatin LAR [4]. Risperdal Consta consists of PLGA microparticles that are loaded with risperidone, a small hydrophobic molecule that is used to treat schizophrenia. Adequate therapeutic levels of risperidone are observed 3 weeks after the first intramuscular injection, followed by a 2-week period of action [4,5]. Sandostatin LAR consists of PLGA-glucose microparticles that are loaded with octreotide acetate, which is the acetate salt of a cyclic octapeptide that is used to treat acromegaly. Adequate therapeutic levels of octreotide acetate are observed 2 weeks after the first intramuscular injection, followed by a 1-month period of action [4,6].

One of the key parameters that governs drug release from PLGA microparticles is the particle size distribution [7]. For instance, the particle size of risperidone PLGA microparticles was shown to affect drug encapsulation efficiency, polymer degradation rate and initial burst release of the drug [8,9]. In general, smaller PLGA microparticles have a higher surface-area-to-volume ratio with more drug molecules on the outer surface that are immediately accessible and a larger surface available for diffusion, resulting in increased release rates [10]. The effect will be more pronounced if the particle porosity is high, since this enhances the particle surface area [11]. Moreover, the presence of larger or agglomerated particles can affect the suspendability and injectability of a product

* Corresponding author at: Division of Drug Delivery Technology, Cluster BioTherapeutics, Leiden Academic Centre for Drug Research, Leiden University, Einsteinweg 55, 2333 CC Leiden, The Netherlands.
E-mail address: w.jiskoot@lacdr.leidenuniv.nl (W. Jiskoot).

http://dx.doi.org/10.1016/j.ejpb.2017.04.002
0939-6411/

[1]. For these reasons, the particle size distribution needs to be accurately controlled during and after manufacturing. Various process parameters are known to affect size and agglomeration of PLGA microparticles. Some factors that seem crucial for the resulting particle size are the volume of organic phase and the method and duration of agitation during the emulsification step [12,13].

The most common techniques to evaluate PLGA microparticle size are optical microscopy, scanning electron microscopy (SEM) and laser diffraction, which have been used since the commercial launch of the first PLGA microparticle drug delivery systems in the 1980s. In addition to particle size information, optical microscopy may also provide information on the tendency of PLGA microparticles to agglomerate [14]. A major drawback of optical microscopy is that it is time-consuming due to manual sample preparation (disposing samples onto slides) and low throughput. Multiple measurements are needed to examine a significant number of microparticles (typically 100–200) allowing calculation of the mean diameter. SEM suffers from similar drawbacks with a laborious sample preparation that may include freeze-drying, optional cross-sectioning, coating and sample mounting, which makes this technique mainly suitable for characterizing surface morphology and internal structure of PLGA microparticles.

By contrast, laser diffraction is less time-consuming owing to a more straightforward sample preparation and a relatively large analysis volume at high sample concentration. The technique is based on a laser beam that is diffracted in a specific pattern depending on the geometrical dimensions of particles in the sample. The particle size distribution is derived from the angle and intensity of the scattered light, which are fitted according to the Fraunhofer and Mie theories [15]. A limitation of laser diffraction is that agglomeration of PLGA microparticles cannot be assessed since samples are not visualized and information on particle morphology is lacking. Thus, the presence of agglomerates may lead to an overestimation of microparticle size.

In this work, we hypothesized that the relatively new technique of flow imaging microscopy could combine the advantages of optical microscopy (visualization of individual particles) and laser diffraction (high throughput). In recent years, flow imaging microscopy has become increasingly popular for the sizing and counting of micron-sized particles in therapeutic protein products [16–18]. In particular, Micro-Flow Imaging (MFI) instruments became well established in the field of subvisible particle analysis [19,20]. In MFI, microscopic images are automatically collected from a sample that passes the optics through a flow cell at a rate that is fast enough to analyze thousands of particles in a few minutes. Particle size is reported as the equivalent circular diameter (ECD), which is the diameter of a circle with the same projected area as the particle. In addition, information on particle count, shape and transparency can be obtained from the analysis software.

The aims of this study were: (1) to evaluate MFI as a tool to accurately assess the size of PLGA microparticles, and (2) to present an approach to detect and quantify PLGA microparticle agglomeration with MFI. For this purpose, we compared MFI with laser diffraction for Risperdal Consta and Sandostatin LAR, and defined the different particle populations detected with MFI. Moreover, we showed two case studies of the application of MFI to support process development of risperidone PLGA microparticles and to study the physical stability of Sandostatin LAR after reconstitution.

2. Materials and methods

2.1. Chemicals

Sodium carboxymethyl cellulose (CMC) and poloxamer 188 were purchased from Sigma-Aldrich, D-mannitol from Applichem, polysorbate 80 from Fagron and polyvinyl alcohol (PVA) 4-88 from Merck. Ultrapure water (≥18 MΩ cm) was obtained from a MilliQ Biocel water purification system (Millipore).

2.2. PLGA microparticles

Risperdal Consta (25-mg vial, Janssen-Cilag B.V., manufactured by Janssen Pharmaceutica, Beerse, Belgium, batch no. EGS6M/EBZUECO/EBSK000, exp. 01/2017) and Sandostatin LAR (30-mg vial, Novartis India, manufactured by Sandoz, Schaftenau, Austria, lot no. S0016, exp. 02/2016) were purchased locally.

Risperidone-loaded poly(lactic-co-glycolic acid) (PLGA) microparticles were prepared by using an oil-in-water (O/W) emulsion solvent extraction method. Samples were taken at different stages during the preparation process. The first sample (“emulsion”) was collected from the O/W emulsion during the solvent extraction step, the second sample (“intermediate”) was collected after concentrating the hardened microparticles over a 25-μm sieve, and the final sample (“final product”) was collected after drying. The final, dried product contained a targeted drug load of 38% (w/w) risperidone microencapsulated in 75:25 (lactide:glycolide) PLGA.

To monitor the physical stability of Sandostatin LAR, a 1.0 mg/ml suspension was prepared in duplicate by dispersing the product in filtered diluent containing 7.0 g/l CMC, 6.0 g/l D-mannitol and 2.0 g/l poloxamer 188. The sample dispersion was homogenized and left at room temperature for at least 20 min until the microparticles visually appeared completely wetted. Next, a 1.0-ml aliquot was removed for MFI analysis (t = 0 h). The remaining sample was divided into two portions. One portion was incubated at 20 °C (room temperature) and one portion at 25 °C (incubator type BD240, Binder) in glass vials (20-ml liquid scintillation vials, Sigma-Aldrich). After 4, 24 and 52 h of incubation, 1.0-ml aliquots were removed for MFI analysis.

2.3. Particle size distribution with Mastersizer

Particle size distributions of Risperdal Consta and Sandostatin LAR were measured by using a Malvern Mastersizer 2000 laser diffraction instrument equipped with a Micro Precision Hydro 2000μP sample dispersion unit (Malvern Instruments). Three measurements were performed per sample and two samples were taken per product. The dispersion unit was drained and flushed with ultrapure water between sample measurements and background detector intensities were checked to ensure cleanliness of the sample compartment.

2.3.1. Mastersizer measurement of Risperdal Consta

Risperdal Consta vials were equilibrated at room temperature for at least 30 min prior to reconstitution. Microparticles (10 mg/ml) were dispersed in 0.01% (w/v) polysorbate 80 and sonicated for 1–2 min. The sample dispersions were measured within 30 min upon preparation and homogenized just before measurement. A sample volume of approximately 2 ml was added into the 20-ml dispersion unit prefilled with ultrapure water and more sample was added until an obscuration level between 5 and 10% was reached. Stirring rate in the dispersion unit was set at 1500 rpm without ultrasonication. The detector array measured the scattering pattern during 20 s.

2.3.2. Mastersizer measurement of Sandostatin LAR

Sandostatin LAR microparticles (24 mg/ml) were dispersed in 0.3% (w/v) polysorbate 80, homogenized and left at room temperature for at least 15 min. The sample dispersions were homogenized again just before measurement. A sample volume of approximately 1 ml was added into the 20-ml dispersion unit

prefilled with ultrapure water and more sample was added until the obscuration level reached a value between 4 and 6%. Stirring rate in the dispersion unit was set at 1200 rpm without ultrasonication. The detector array measured the scattering pattern during 30 s.

2.3.3. Mastersizer data analysis

The Mastersizer raw data were analyzed with the Malvern Mastersizer 2000 software (version 5.22) using the Fraunhofer model ($n_{dispersant}$ = 1.330), general purpose mode, normal calculation sensitivity and assuming an irregular particle shape. Number and volume % results were exported for particle sizes ranging from 2 to 222 μm with a bin size of 4 μm. Number and volume percentiles, spans, surface mean d[3,2] and volume mean d[4,3] were obtained from the software. Volume-based particle size distributions were fitted with a medium Lowess curve (with a smoothing window of 10 points) in GraphPad Prism 5 (version 5.02) to determine the volume mode.

2.4. Particle size distribution with Micro-Flow Imaging (MFI)

MFI measurements were performed with an MFI 5100 instrument (featuring a flow cell depth of 400 μm) equipped with a high-throughput BOT1 autosampler (ProteinSimple). Data were acquired with MFI View System Software (MVSS) version 2-R4 and processed with MFI View Analysis Suite (MVAS) software version 1.4.0. Sample diluents were filtered through a Millex-GP 0.22-μm sterile syringe filter (Millipore). A baseline measurement was performed with sample diluent to ensure that less than 500 particles/ml were present. Optimize illumination was performed on the sample diluent and samples were stirred 12 times at a speed of 6 before they were introduced into the sample port. The sample purge volume was set at 0.20 ml and the analyzed sample volume was 0.571 ml. At least 3000 particles were analyzed per measurement and samples were measured in triplicate. The reported particle size (in μm) is the equivalent circular diameter (ECD) detected by MFI.

2.4.1. MFI sample preparation

Risperdal Consta (1.0 mg/ml) and the final, dried product of risperidone PLGA microparticles (1.0 mg/ml) were dispersed in filtered diluent containing 0.5% (w/v) polysorbate 80. Sandostatin LAR (0.5 mg/ml) was dispersed in filtered diluent containing 7.0 g/l CMC, 6.0 g/l D-mannitol and 2.0 g/l poloxamer 188. The sample dispersions were homogenized and left at room temperature for at least 20 min until the microparticles visually appeared completely wetted. Emulsion and intermediate samples of risperidone PLGA microparticles were diluted in 5% (w/v) PVA 4–88 until less than 13,000 particles were analyzed per measurement. The samples were homogenized just before transferring 1.0 ml to a 96-well plate (Eppendorf) suitable for the Bot1 autosampler.

2.4.2. MFI data analysis

Edge particles were removed from MFI raw data with the MVAS software. Number and volume % results were exported for particle sizes ranging from 2 to 222 μm with a bin size of 4 μm. Number percentiles were obtained from the software. Volume percentiles were determined from the cumulative size distribution curve, where D_v10, D_v50 and D_v90 percentiles are the diameters at 10%, 50%, and 90% cumulative particle volume, respectively. The width of the number- and volume-based size distributions was calculated as the span according to Eqs. (1) and (2):

$$\text{Number span} = \frac{(D_n90 - D_n10)}{(D_n50)} \quad (1)$$

$$\text{Volume span} = \frac{(D_v90 - D_v10)}{(D_v50)} \quad (2)$$

The surface mean d[3,2] and volume mean d[4,3] were calculated from MFI data of individual particles according to Eqs. (3) and (4):

$$d[3,2] = \frac{\sum D_i^3}{\sum D_i^2} \quad (3)$$

$$d[4,3] = \frac{\sum D_i^4}{\sum D_i^3} \quad (4)$$

where: D_i = ECD of the *i*th particle.

Volume-based size distributions were fitted by using GraphPad Prism with a medium Lowess curve (10-points smoothing window) to determine the volume mode. The cumulative particle volume and surface were calculated and divided by the number of measured particles to obtain the mean particle volume and surface.

2.4.3. Particle classification

By using the filter manager in the MVAS software, ECD and aspect ratio cutoffs were set to distinguish three different particle populations: "fines", "monospheres" and "agglomerates". A customized filter was defined for each PLGA microparticle product (Fig. 1). For Risperdal Consta and intermediate and final product samples of risperidone PLGA microparticles, filter cutoffs were

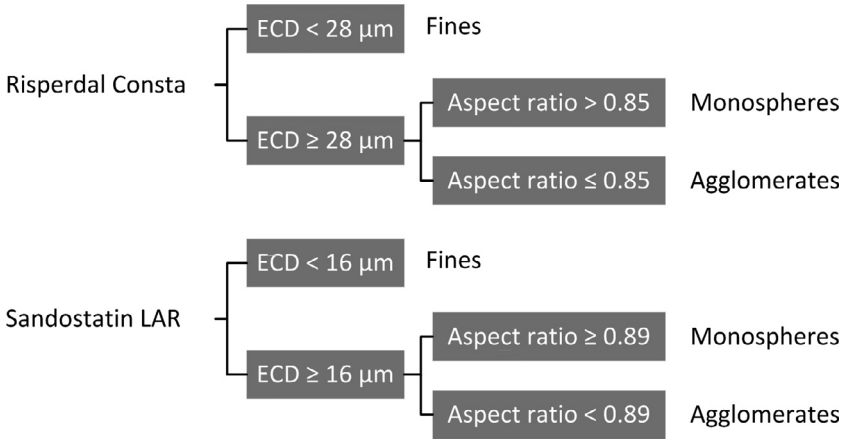

Fig. 1. MVAS filter manager settings for Risperdal Consta and Sandostatin LAR developed to classify particles according to three categories: fines, monospheres and agglomerates. For in-house produced risperidone PLGA microparticles, the Risperdal Consta filter settings were used.

set at an ECD of 28 μm and an aspect ratio of 0.85. For Sandostatin LAR, filter cutoffs were set at an ECD of 16 μm and an aspect ratio of 0.89. Application of the customized filters, as shown in Fig. 1, was followed by visual examination of particle images of the monospheres population to identify and select any additional agglomerates that were misclassified as monospheres. Manual selection of agglomerated particles within the monospheres population resulted in 0.1–2.7 vol% of additional agglomerates.

3. Results and discussion

3.1. Particle size distributions obtained with MFI versus Mastersizer

Two commercial PLGA microparticle products, Risperdal Consta and Sandostatin LAR, were characterized by using the established Mastersizer technique and the relatively novel technique of MFI (Fig. 2). While MFI detects individual particles and thus provides primarily number-based results, these can be converted to volume-based results by assuming spherically shaped particles. The Mastersizer instrument uses the volume of particles to determine their diameter, but the fundamental volume distribution can be transformed to number distribution, also by assuming spherical particles, with the Mastersizer 2000 software. In order to compare MFI with Mastersizer results, particle size distributions are presented in number % (Fig. 2A and C) as well as volume % (Fig. 2B and D).

Number and volume size distributions measured with Mastersizer and MFI were substantially similar for the main particle fraction of Risperdal Consta (between 28 μm and 220 μm) and Sandostastin LAR (between 16 μm and 124 μm). However, an additional fraction of smaller particles (<28 μm for Risperdal Consta and <16 μm for Sandostatin LAR) was clearly visible with MFI, but not with Mastersizer, in the number-based size distribution (Fig. 2A and C). Also, modelling the Mastersizer raw data according

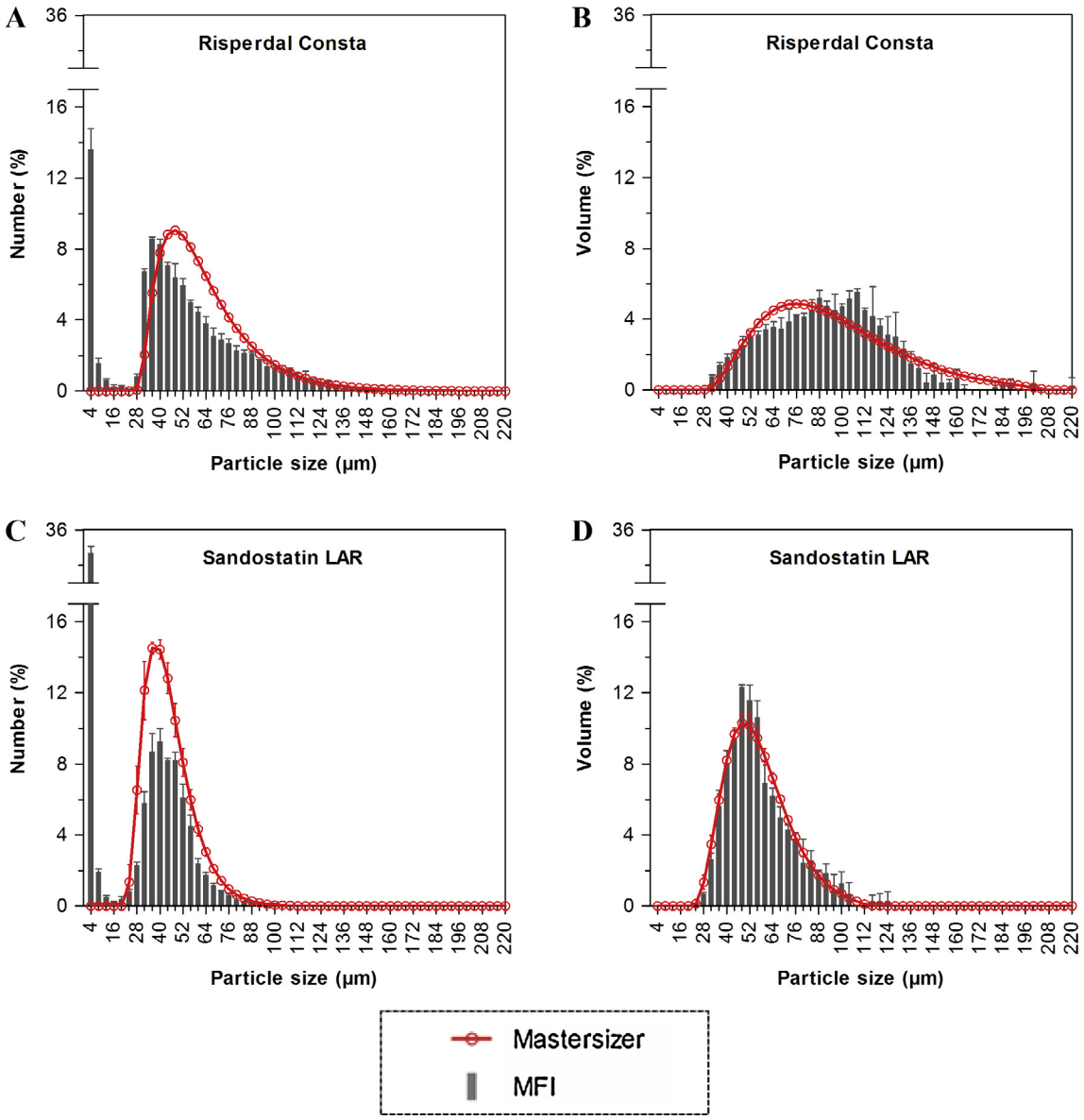

Fig. 2. Particle size distributions of (A, B) Risperdal Consta and (C, D) Sandostatin LAR measured with Mastersizer (red curve) and Micro-Flow Imaging (MFI, grey size bins). For each particle size, the corresponding (A, C) number and (B, D) volume percentages are shown. Mastersizer results are the mean of two samples each measured in triplicate (±standard deviation). MFI results are the mean of three samples (+standard deviation). (For interpretation of the references to color in this figure legend, the reader is referred to the web version of this article.)

Table 1
Particle size distribution characteristics of Risperdal Consta and Sandostatin LAR measured with Mastersizer and Micro-Flow Imaging (MFI). Number and volume percentiles and span values are shown, as well as other relevant particle size distribution characteristics that can be calculated from Mastersizer and/or MFI data. Mastersizer results are the mean of two samples each measured in triplicate (±standard deviation). MFI results are the mean of three samples (±standard deviation).

	Risperdal Consta		Sandostatin LAR	
	Mastersizer	MFI	Mastersizer	MFI
Number percentiles				
D_n10 (μm)	39.3 ± 0.9	3.6 ± 0.4	30.9 ± 1.0	2.1 ± 0.0
D_n50 (μm)	57.9 ± 0.9	47.4 ± 0.8	42.3 ± 1.1	35.7 ± 0.5
D_n90 (μm)	94.4 ± 0.8	92.5 ± 2.5	61.3 ± 0.3	56.2 ± 0.2
Number span	0.95 ± 0.02	1.88 ± 0.02	0.72 ± 0.04	1.52 ± 0.02
Volume percentiles				
D_v10 (μm)	54.0 ± 0.6	51.3 ± 1.1	37.5 ± 0.8	38.4 ± 0.7
D_v50 (μm)	89.1 ± 0.3	92.3 ± 2.9	54.3 ± 0.1	53.5 ± 0.4
D_v90 (μm)	143.0 ± 0.0	129.5 ± 3.4	79.0 ± 2.0	80.7 ± 2.7
Volume span	1.00 ± 0.01	0.85 ± 0.02	0.77 ± 0.05	0.79 ± 0.04
Other characteristics				
Surface mean d[3,2] (μm)	82.5 ± 0.5	81.1 ± 2.6	52.1 ± 0.1	52.6 ± 0.7
Volume mean d[4,3] (μm)	94.4 ± 0.3	92.3 ± 3.8	56.6 ± 0.4	57.2 ± 0.7
Volume mode (μm)	76.0 ± 0.0	101.3 ± 5.9	48.4 ± 0.0	48.4 ± 0.0
Cumulative surface (mm^2)	Not available with Mastersizer	47.0 ± 4.6	Not available with Mastersizer	13.5 ± 0.9
Cumulative volume (μl)		0.64 ± 0.08		0.12 ± 0.01
Particle concentration (#/ml)		7505 ± 379		5359 ± 169
Total number of particles		4286 ± 216		3061 ± 97
Mean particle surface (mm^2)		0.011 ± 0.001		0.004 ± 0.000
Mean particle volume (nl)		0.148 ± 0.012		0.039 ± 0.002

to the Mie instead of Fraunhofer theory or using the analysis model "multiple narrow modes" instead of the "general purpose mode" did not allow detection of the smaller particles in presence of the main PLGA microparticle fraction (data not shown).

This discrepancy between Mastersizer and MFI was reflected in the number percentiles and number span values calculated for both products, while volume percentiles and volume span values corresponded well between the two techniques (Table 1). In particular, the D_n10 values measured with MFI were much smaller than those measured with Mastersizer (3.6 ± 0.4 μm *vs.* 39.3 ± 0.9 μm for Risperdal Consta; 2.1 ± 0.0 μm *vs.* 30.9 ± 1.0 μm for Sandostatin LAR), because Mastersizer did not detect the smaller particle fraction. Accordingly, number span values reported by MFI were significantly larger than those reported by Mastersizer (1.88 ± 0.02 *vs.* 0.95 ± 0.02 for Risperdal Consta; 1.52 ± 0.02 *vs.* 0.72 ± 0.04 for Sandostatin LAR), due to the wider number size distribution detected with MFI.

A similar observation was done by Farrell et al. [21], who analyzed cell culture microcarriers with Mastersizer and MFI. The researchers showed that MFI was able to detect smaller particles (<50 μm) that were overlooked by Mastersizer in presence of larger particles (with an average ECD of 176 μm), and explained this by the difference in measurement principle (i.e., number-based *versus* volume-based). Smaller particles are probably missed by the Mastersizer because the light scattering signal, which relates to volume % rather than number %, is dominated by the larger particles. In addition, Mastersizer measures all particles simultaneously and gives an approximate representation of the volume distribution, whereas MFI measures individual particles [21]. This also explains why our Mastersizer results appear as smooth averaged curves, while MFI results are much more affected by the presence of individual particles (Fig. 2).

The particle sizes of Risperdal Consta reported in the literature lay between 25 and 150 μm [22], with an approximate average size of 0.1 mm [23], and the reported average size of Sandostatin LAR detected by scanning electron microscopy is about 50 μm [24]. The volume means d[4,3] of Risperdal Consta and Sandostatin LAR that we measured with MFI (92.3 ± 3.8 μm and 57.2 ± 0.7 μm, respectively) closely match those measured with

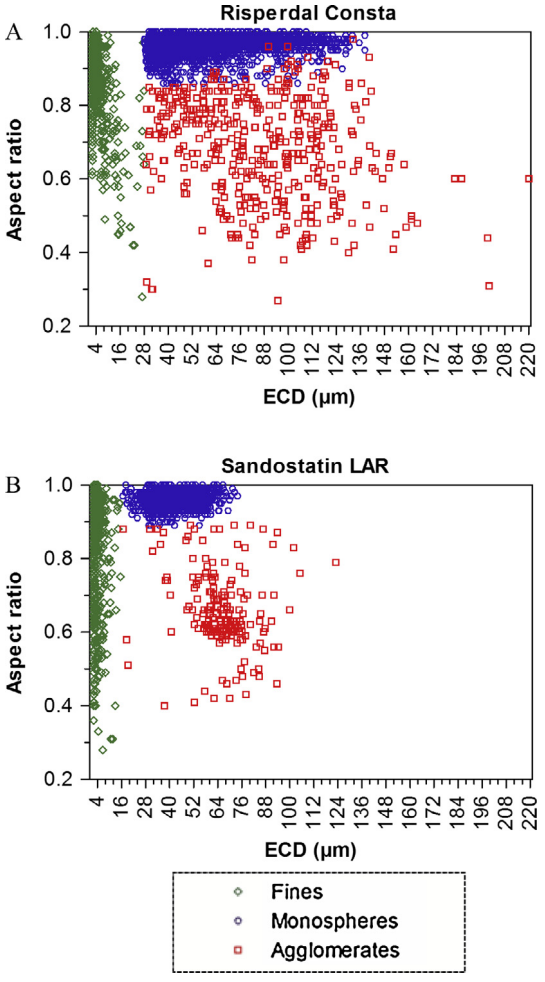

Fig. 3. Scatter plots with the aspect ratio and equivalent circular diameter (ECD) of particles in individual samples of (A) Risperdal Consta and (B) Sandostatin LAR measured with Micro-Flow Imaging (MFI).

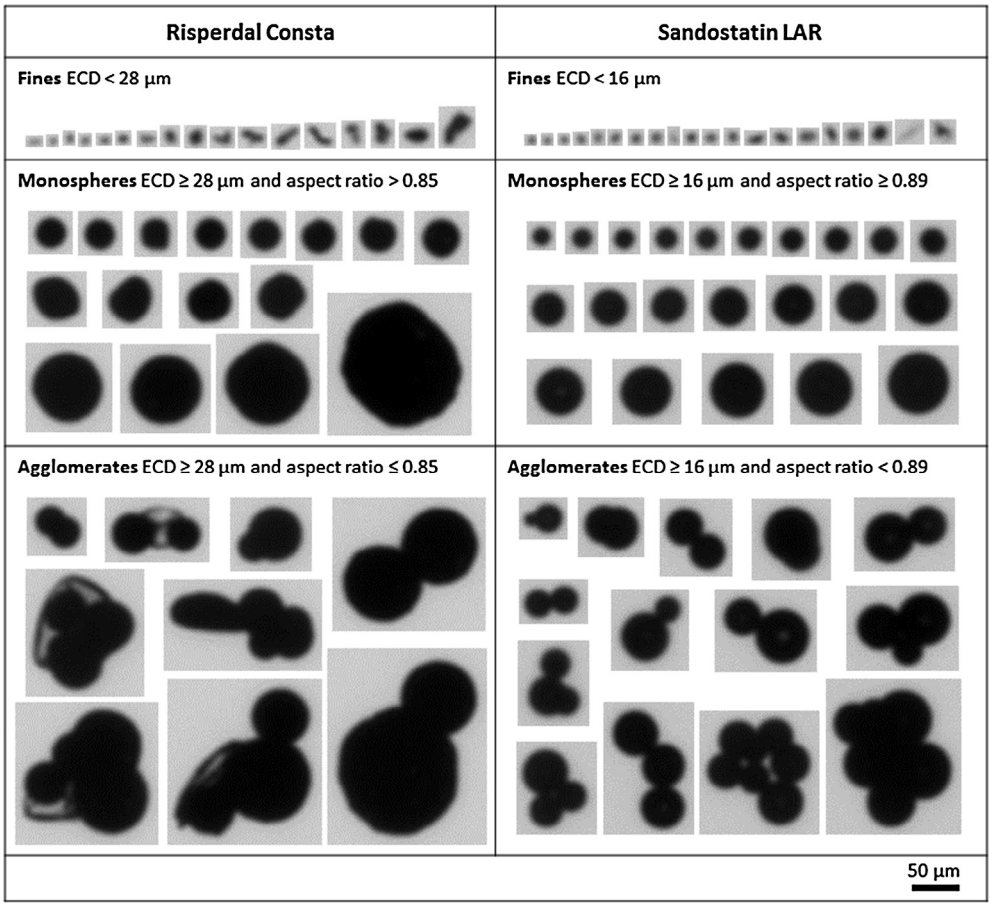

Fig. 4. Exemplary images of particles in Risperdal Consta and Sandostatin LAR captured with Micro-Flow Imaging (MFI). Particles are divided into three different categories, i.e., fines, monospheres and agglomerates, based on their equivalent circular diameter (ECD) and aspect ratio provided by the MFI View Analysis Suite (MVAS) software.

Mastersizer (94.4 ± 0.3 µm and 56.6 ± 0.4 µm, respectively) (Table 1), and also agree with literature values. Importantly, MFI provides additional number-based information that is not available with Mastersizer such as particle concentration, mean particle surface and mean particle volume (Table 1). Moreover, MFI shows higher sensitivity towards sample-to-sample or batch-to-batch variations owing to its ability to measure individual particles and provide information about their morphology (see Section 3.2). These major advantages can be of great importance for the purpose of pharmaceutical development and quality control of PLGA microparticle products.

3.2. Particle classification with MFI in Risperdal Consta and Sandostatin LAR

MFI, as an imaging technique, not only provides the ECD of individual particles, but also gives information on particle morphology. One of those morphological parameters is the aspect ratio, defined as "the ratio of the minor axis length over the major axis length of an ellipse that has the same second-moments as the particle" with values ranging from 0 to 1 (no units; 1 for a perfect circle) [25]. Based on a scatter plot of aspect ratio as a function of ECD, three distinct particle populations could be distinguished in Risperdal Consta and Sandostatin LAR (Fig. 3).

The population defined as "fines" consisted of the smaller particle fraction (<28 µm for Risperdal Consta and <16 µm for Sandostatin LAR) and displayed a wide range of aspect ratios from 0.28 to 1, which suggests that the shape of these particles varied from rod-like or fibrous to perfectly spherical. Particle images corresponding to the fines captured by MFI indeed showed a wide variety of shapes (Fig. 4). A clear size gap was present in the scatter plots of both products between the fines and two other populations, i.e., "monospheres" and "agglomerates". Monospheres appeared to be close to spherical with aspect ratios >0.85 for Risperdal Consta and ≥0.89 for Sandostatin LAR, whereas agglomerates consisted of multiple spheres resulting in lower aspect ratios (Figs. 3 and 4).

A filter was developed in MVAS based on the mentioned ECD and aspect ratio cutoffs (Fig. 1). To verify the ability of the filter to distinguish agglomerates from monospheres, the images of particles defined as monospheres were visually examined. In general, this resulted in the identification of a few volume percent of additional agglomerates with high aspect ratios (>0.85), such as the agglomerates (red[1] open squares) that can be seen within the monospheres population (blue open circles) in Risperdal Consta (Fig. 3A). Based on the MVAS filters combined with visual examination, separate number and volume size distributions could be generated for the fines, monospheres and agglomerates in Risperdal Consta and Sandostatin LAR (Fig. 5). Also, the number %, volume %, D_v50, volume span and volume mode were calculated for each particle population (Table 2).

Although the fines contributed considerably to the total number of particles (16.5 ± 0.9% and 37.2 ± 0.4%, respectively for Risperdal Consta and Sandostatin LAR), their contribution to the total particle volume was negligible (<0.05% for both products). The nature of these fines could be extrinsic (contaminants), intrinsic (related to the drug product) or inherent (originating from the drug product)

[1] For interpretation of color in Figs. 3 and 9, the reader is referred to the web version of this article.

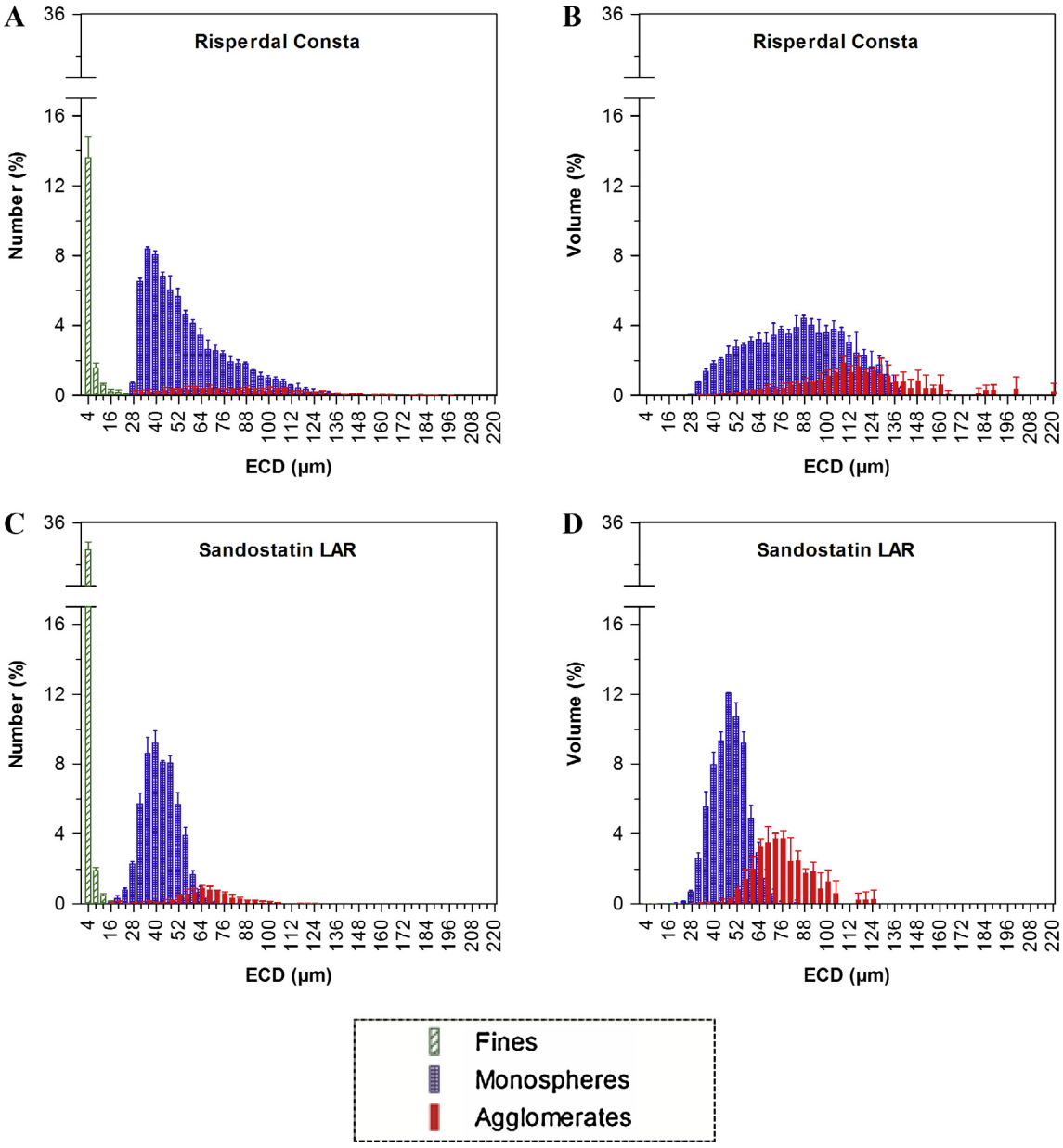

Fig. 5. Particle size distributions of the different populations (i.e., fines, monospheres and agglomerates) in (A, B) Risperdal Consta and (C, D) Sandostatin LAR measured with Micro-Flow Imaging. Size distributions are shown as (A, C) number and (B, D) volume percentages. Results are the mean of three samples (+standard deviation).

[16]. We cannot exclude that some of the fines consisted of extrinsic particles, such as dust or hair fragments, that contaminated the sample during sample preparation or MFI measurement. As a control, baseline measurements were performed with sample diluent, which generally showed particle concentrations that were 5–10 times lower than the fines population in commercial PLGA microparticle samples (data not shown). Thus, most likely mainly intrinsic and/or inherent particles were present in the fines population. In the case of cell culture microcarriers, researchers suggested that the main particle fraction was accompanied by a smaller particle fraction originating from debris produced during manufacturing of the microcarriers [21]. In the case of PLGA microparticles, debris in the form of fine PLGA particles or fragments may have been formed during the Risperdal Consta and Sandostatin LAR manufacturing processes.

The main particle population produced during manufacturing consisted of monospheres with a D_v50 of 85.1 ± 1.1 µm for Risperdal Consta and 48.5 ± 0.5 µm for Sandostatin LAR (Table 2). Risperdal Consta monospheres showed slightly lower aspect ratios and broader size distributions (span value 0.83 ± 0.03) than Sandostatin LAR monospheres (span value 0.48 ± 0.02). Besides fines and monospheres, a considerable volume fraction of agglomerated PLGA microparticles was present in Risperdal Consta (25.1 ± 3.8%) and Sandostatin LAR (31.4 ± 1.7%). These agglomerates may have been formed during manufacturing and/or storage of the products. Moreover, Risperdal Consta agglomerates generally consisted of two or three PLGA microparticles that were slightly misshaped, whereas Sandostatin LAR agglomerates consisted of two, three or multiple PLGA microparticles that were nearly spherical (Fig. 4). These differences in particle characteristics may be the result of the different encapsulation techniques associated with the two commercial products, i.e., O/W emulsion solvent extraction for Risperdal Consta and coacervation for Sandostatin LAR [26]. Also, PLGA properties (such as PLGA *versus* PLGA-glucose star polymer, co-monomer ratio, molecular weight), drug properties of risperidone (a small hydrophobic molecule)

Table 2
Particle size distribution characteristics of the different populations (i.e., fines, monospheres and agglomerates) in Risperdal Consta and Sandostatin LAR measured with Micro-Flow Imaging. The number percentage, volume percentage, median particle size (D_v50), volume span, and volume mode of each population are shown. Results are the mean of three samples (±standard deviation).

		Risperdal Consta	Sandostatin LAR
Fines	Number %	16.5 ± 0.9	37.2 ± 0.4
	Volume %	<0.05	<0.05
	D_v50 (μm)	20.0 ± 2.0	8.0 ± 0.4
	Volume span	1.01 ± 0.12	1.39 ± 0.04
	Volume mode (μm)	18.5 ± 2.3	12.7 ± 0.5
Monospheres	Number %	75.4 ± 0.8	55.9 ± 0.3
	Volume %	74.9 ± 3.9	68.5 ± 1.6
	D_v50 (μm)	85.1 ± 1.1	48.5 ± 0.5
	Volume span	0.83 ± 0.03	0.48 ± 0.02
	Volume mode (μm)	90.8 ± 7.8	46.4 ± 1.7
Agglomerates	Number %	8.2 ± 0.9	6.9 ± 0.5
	Volume %	25.1 ± 3.8	31.4 ± 1.7
	D_v50 (μm)	114.3 ± 5.2	74.1 ± 1.7
	Volume span	0.66 ± 0.08	0.51 ± 0.03
	Volume mode (μm)	112.2 ± 4.0	70.7 ± 2.3

versus octreotide acetate (acetate salt of a cyclic octapeptide), formulation of the product and storage conditions can have an effect on the size distribution and agglomeration behavior of the microparticles.

In general, formulation and process parameters as well as storage conditions can have a large impact on the size characteristics of PLGA microparticles, affecting the drug release profile and thus the efficacy and safety in patients. Our results show that MFI is an excellent tool for in-depth PLGA microparticle characterization. Not only the size distribution and morphology of the main particle population (monospheres) can be assessed, but MFI also enables us to distinguish and quantify other populations such as fines and agglomerates.

3.3. Case study 1: process development of risperidone PLGA microparticles

Here, we present an example of applying MFI as a tool to monitor particle size and agglomeration during the manufacturing process of a PLGA microparticle product. One batch of risperidone loaded PLGA microparticles was prepared in-house by using an O/W emulsion solvent extraction method. Formulation and process parameters were chosen to obtain a final product with similar properties as Risperdal Consta (38% (w/w) drug loading, 75:25 (lactide:glycolide) PLGA, and similar particle size distribution). To study the effect of certain process steps on particle characteristics, samples were taken at three different stages during the preparation of risperidone PLGA microparticles and measured off-line with MFI.

The first sample ("emulsion") was collected during the solvent extraction step after emulsification. During emulsification, the organic phase containing risperidone and PLGA was mixed with an aqueous, continuous phase in presence of a stabilizing agent to form emulsion droplets. Subsequently, the O/W emulsion was added to a large volume of aqueous phase to remove solvent from the emulsion droplets (solvent extraction). The size distribution of the emulsion droplets, which are the precursors of microparticles, may depend on stabilizer concentration, viscosity, mixing time, and amount of shear applied during emulsification [7,12,27,28]. For example, the speed of stirring during emulsification was shown to affect particle size and the extent of agglomeration in the final, lyophilized PLGA microparticle product [29]. Thus, process parameters during the emulsification phase will provide a basis for the size distribution of the final product.

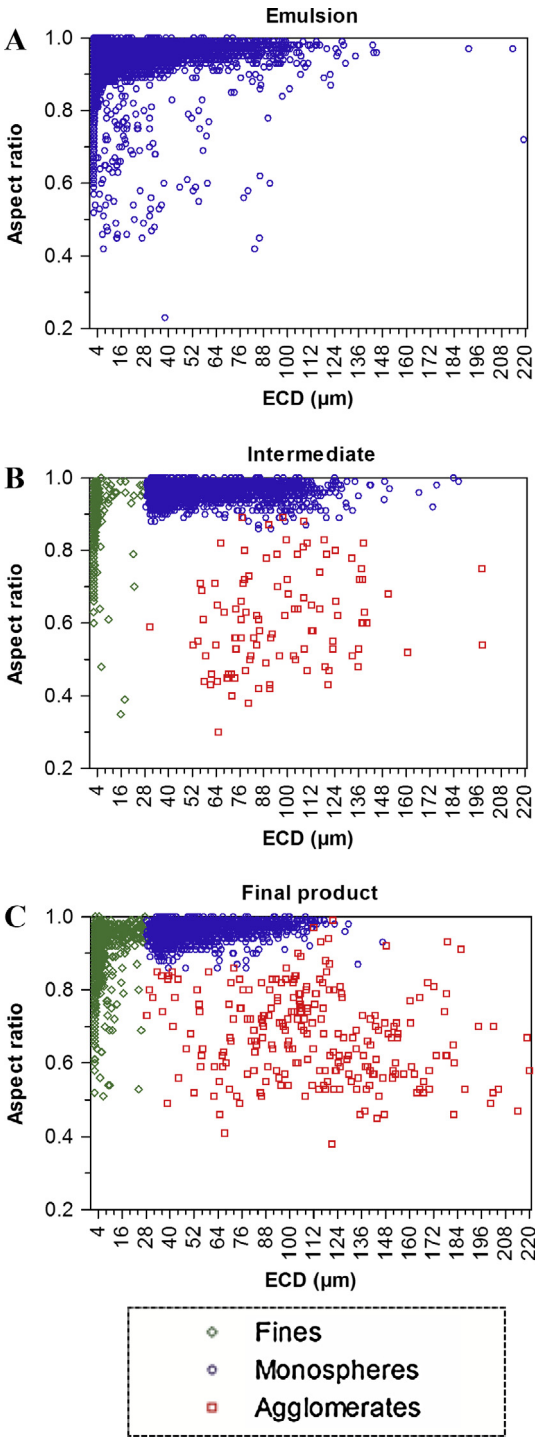

Fig. 6. Scatter plots with the aspect ratio and equivalent circular diameter (ECD) of particles in the (A) emulsion, (B) intermediate, and (C) final product of risperidone PLGA microparticles measured with Micro-Flow Imaging.

Interestingly, the emulsion droplets in our sample did not show distinct particle populations according to the scatter plot (Fig. 6A). There was no size gap present at lower ECD values in the particle size distribution (Fig. 7A and B), indicating that a distinct fines population was not present yet at this stage of the manufacturing process. Moreover, emulsion droplets in the full ECD range appeared as individual spheres and examination of MFI images did not reveal any agglomerates. An explanation for the absence of agglomerates may be that if one emulsion droplet encounters another droplet,

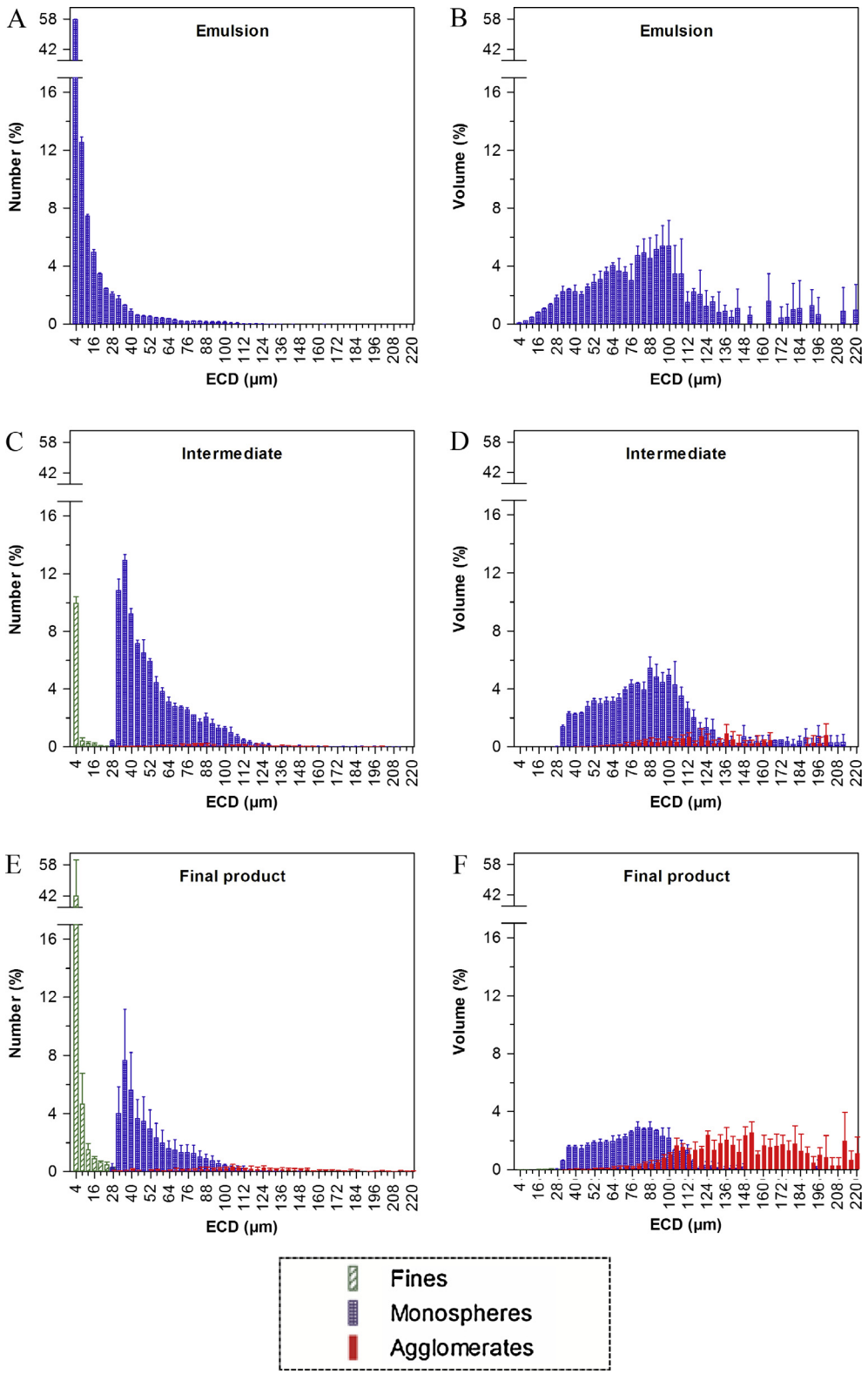

Fig. 7. Particle size distributions of the different populations (i.e. fines, monospheres and agglomerates) in the (A, B) emulsion, (C, D) intermediate, and (E, F) final product of risperidone PLGA microparticles measured with Micro-Flow Imaging. Size distributions are shown as (A, C, E) number and (B, D, F) volume percentages. Results are the mean of three samples (+standard deviation).

they will easily merge to form a larger droplet. Thus, the emulsion sample consisted of monospheres only with a D_v50 of 86.5 ± 3.7 µm and a relatively wide volume span of 1.58 ± 0.53 (Table 3).

The second sample ("intermediate") contained wet microparticles collected on a 25-µm sieve after the solvent extraction step (Fig. 6B). Solvent removal caused the emulsion droplets to solidify and form hardened microparticles. Particle size and morphology

Table 3
Particle size distribution characteristics of the different populations (i.e. fines, monospheres and agglomerates) in the emulsion, intermediate, and final product of risperidone PLGA microparticles measured with Micro-Flow Imaging. The number percentage, volume percentage, median particle size (D_v50), volume span and volume mode of each population are shown. Results are the mean of three samples (±standard deviation).

		Emulsion	Intermediate	Final product
Total	D_v50 (μm)	86.5 ± 3.7	89.3 ± 1.4	112.3 ± 1.7
	Volume span	1.58 ± 0.53	1.16 ± 0.26	1.47 ± 0.07
	Volume mode (μm)	87.8 ± 3.9	88.2 ± 0.6	86.8 ± 6.5
Fines	Number %	No fines detected	11.1 ± 0.7	50.6 ± 21.0
	Volume %		<0.05	0.1 ± 0.1
	D_v50 (μm)		23.9 ± 1.3	20.0 ± 2.8
	Volume span		0.73 ± 0.04	0.91 ± 0.22
	Volume mode (μm)		23.7 ± 0.0	17.5 ± 2.1
Monospheres	Number %	100.0 ± 0.0	86.5 ± 0.6	43.8 ± 18.6
	Volume %	100.0 ± 0.0	87.9 ± 0.1	43.8 ± 1.2
	D_v50 (μm)	86.5 ± 3.7	86.1 ± 0.9	78.3 ± 1.2
	Volume span	1.58 ± 0.53	0.99 ± 0.15	0.81 ± 0.03
	Volume mode (μm)	87.8 ± 3.9	88.2 ± 0.6	82.6 ± 4.6
Agglomerates	Number %	No agglomerates detected	2.4 ± 0.3	5.6 ± 2.4
	Volume %		12.1 ± 0.2	56.1 ± 1.2
	D_v50 (μm)		133.2 ± 19.2	155.6 ± 2.0
	Volume span		0.91 ± 0.05	0.87 ± 0.07
	Volume mode (μm)		141.4 ± 12.7	140.1 ± 7.9

can be affected by the rate of solvent extraction, which is controlled by the aqueous phase composition, co-solvent concentration, solid-to-liquid ratio, temperature, and stirring speed [30,31]. The scatter plot of our intermediate sample revealed the presence of the same three types of particle populations as described in the previous section, i.e., fines, monospheres and agglomerates (Fig. 6B).

The corresponding number size distribution indicated that the total number percentage of particles smaller than 28 μm in the intermediate sample was much lower than in the emulsion sample, and the intermediate sample also showed a clear size gap between the fines and monospheres population (Fig. 7C). This is probably because the sieving step removed many particles smaller than 25 μm, but not all of them. The efficiency of sieving may not be 100% due to adherence of small particles to the surface of larger particles that are unable to travel through the sieve. This type of sieving might also explain the presence of the fines population in the two commercial products, Risperdal Consta and Sandostatin LAR.

Importantly, the solvent extraction and wet sieving step did not seem to affect the D_v50 of the monospheres (emulsion 86.5 ± 3.7 μm; intermediate 86.1 ± 0.9 μm), but it caused the formation of 12.1 ± 0.2 vol% of agglomerates with a D_v50 of 133.2 ± 19.2 μm (Table 3). There may be several reasons for agglomeration at this stage. One possible reason may be that the microparticles were not fully solidified due to a relatively high residual solvent content, resulting in a higher tendency to agglomerate in the concentrating and sieving process [7,13,31,32]. Also, a stabilizer concentration that is too high may result in an increased number of agglomerated microparticles during solidification [26].

Lastly, a sample of the final, dried product was measured with MFI (Fig. 6C). Again, the three particle populations could clearly be detected (Fig. 7E). Although the fines did not significantly contribute to the volume distribution (Fig. 7F), the number percentage of fines was enhanced in the final product (50.6 ± 21.0%) compared with the intermediate sample (11.1 ± 0.7%) (Table 3). A reason for this may be that additional fines could have been released from larger particles during the final drying step, which included shear forces.

Furthermore, an increase in the D_v50 of the total particle population was observed compared with the intermediate sample (intermediate 89.3 ± 1.4 μm; final product 112.3 ± 1.7 μm) (Table 3). The increase in the D_v50 of the total particle population could not be explained by a growth in the size of the microparticles, but was due to a remarkable increase in volume percentage of agglomerates (intermediate 12.1 ± 0.2%; final product 56.1 ± 1.2%). The D_v50 of the monospheres population even decreased (intermediate 86.1 ± 0.9 μm; final product 78.3 ± 1.2 μm), likely due to shrinkage of the particles upon drying. It is clear that, in our case study, the final drying step was primarily responsible for the high degree of agglomeration. With this knowledge one may be able to adjust the process parameters in order to prevent agglomeration. For instance, the use of an aqueous solution of mannitol was reported to prevent agglomeration upon freeze-drying of risperidone PLGA microparticles [8].

In summary, MFI provides detailed insight into the impact of successive process steps on PLGA microparticle characteristics. More specific, microparticle size and the formation of different particle populations can be followed during the preparation process. Information obtained with this technique provides a basis for finding the right process parameters to achieve an optimal particle size distribution that gives the desired suspendability, injectability and release kinetics.

In this case study we have shown results from off-line MFI analyses, but in future applications it may even be possible to deploy MFI for on-line measurements. Following a quality-by-design approach, one could imagine employing MFI as process analytical technology tool during PLGA microparticle manufacturing [33], e.g., to decide when to stop the emulsification process (at steady state or at the desired droplet size). Moreover, it seems to be a suitable and relatively straightforward method for the purpose of quality control.

3.4. Case study 2: monitoring the physical stability of Sandostatin LAR

In addition to manufacturing process parameters, it is important to assess the impact of transport, storage and handling on the (particle) characteristics of PLGA microparticle products, since these may significantly impact product quality. For this reason, the physical stability of PLGA microparticle products should be evaluated before and after reconstitution.

Sandostatin LAR dry powder is relatively stable for a prolonged period of time at 2–8 °C, or for at least 1 h at room temperature [6]. However, after mixing the Sandostatin LAR dry powder with the diluent, the drug suspension must be administered immediately (within 2–3 min) because of the high tendency of the microparticles to agglomerate after reconstitution [6,34]. In case of microparticle agglomeration, it becomes difficult or even impossible to

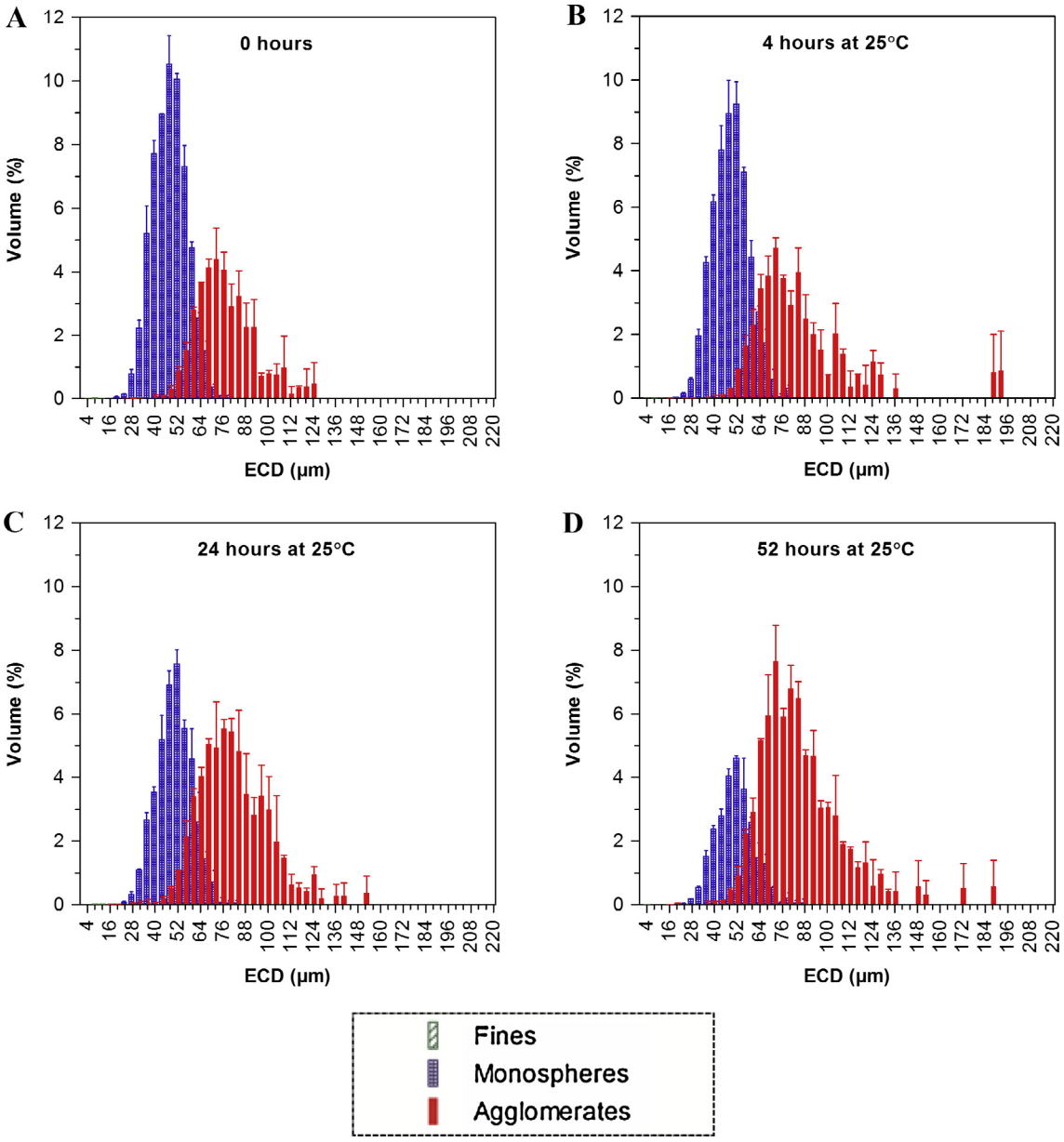

Fig. 8. Volume-based particle size distributions of Sandostatin LAR measured with Micro-Flow Imaging during incubation at 25 °C. Samples were analyzed after reconstitution at (A) 0 h, and after incubation of the reconstituted product for (B) 4 h, (C) 24 h, and (D) 52 h at 25 °C. Results are the mean of two samples (+standard deviation). Incubation of reconstituted Sandostatin LAR at 20 °C for 4, 24 and 52 h did not result in a significant change in the size distribution (data not shown).

inject the Sandostatin LAR drug suspension, leading to product loss. This is in sharp contrast with Risperdal Consta, which can be kept at 25 °C for up to 6 h after reconstitution without injectability issues [35]. In this case study, we evaluated the physical stability of Sandostatin LAR after reconstitution, by monitoring particle size and agglomeration in time with MFI.

Directly after reconstitution and complete suspension of the drug product, a first baseline MFI measurement (0 h) was performed (Fig. 8A). The volume-based particle size distributions of fines, monospheres and agglomerates corresponded well with those previously measured in Sandostatin LAR (Fig. 5D). After 4 h of incubation at 25 °C, several larger agglomerates (>124 µm) were formed and the volume percentage of agglomerates in the complete size range appeared to increase, while the volume percentage of monospheres decreased (Fig. 8B). A further increase in volume percentage of agglomerates and a concomitant decrease in volume percentage of monospheres were apparent at 24 and 52 h (Fig. 8C and D). In contrast, no significant changes were observed over time in the size distributions of the fines, monospheres and agglomerates during incubation of reconstituted Sandostatin LAR at 20 °C for up to 52 h (data not shown).

Importantly, incubation at 25 °C resulted in a significant decrease in the total particle concentration, expressed as number of particles per ml (Fig. 9A, black line, closed triangles). This was caused by a decrease in the number of monospheres (Fig. 9A, blue line, closed circles), which logically was relatively large compared with the smaller increase in the number of agglomerates (Fig. 9A, red line, closed squares). This implies that two or more monospheres attached to each other to form one agglomerate. Ongoing agglomeration also resulted in a significantly larger volume span of the agglomerates at 52 h than at 0 h, pointing to widening of the size distribution for this population (Fig. 9B).

The median particle size (D_v50) of the total particle population shifted to larger sizes in the course of time, which was not due to

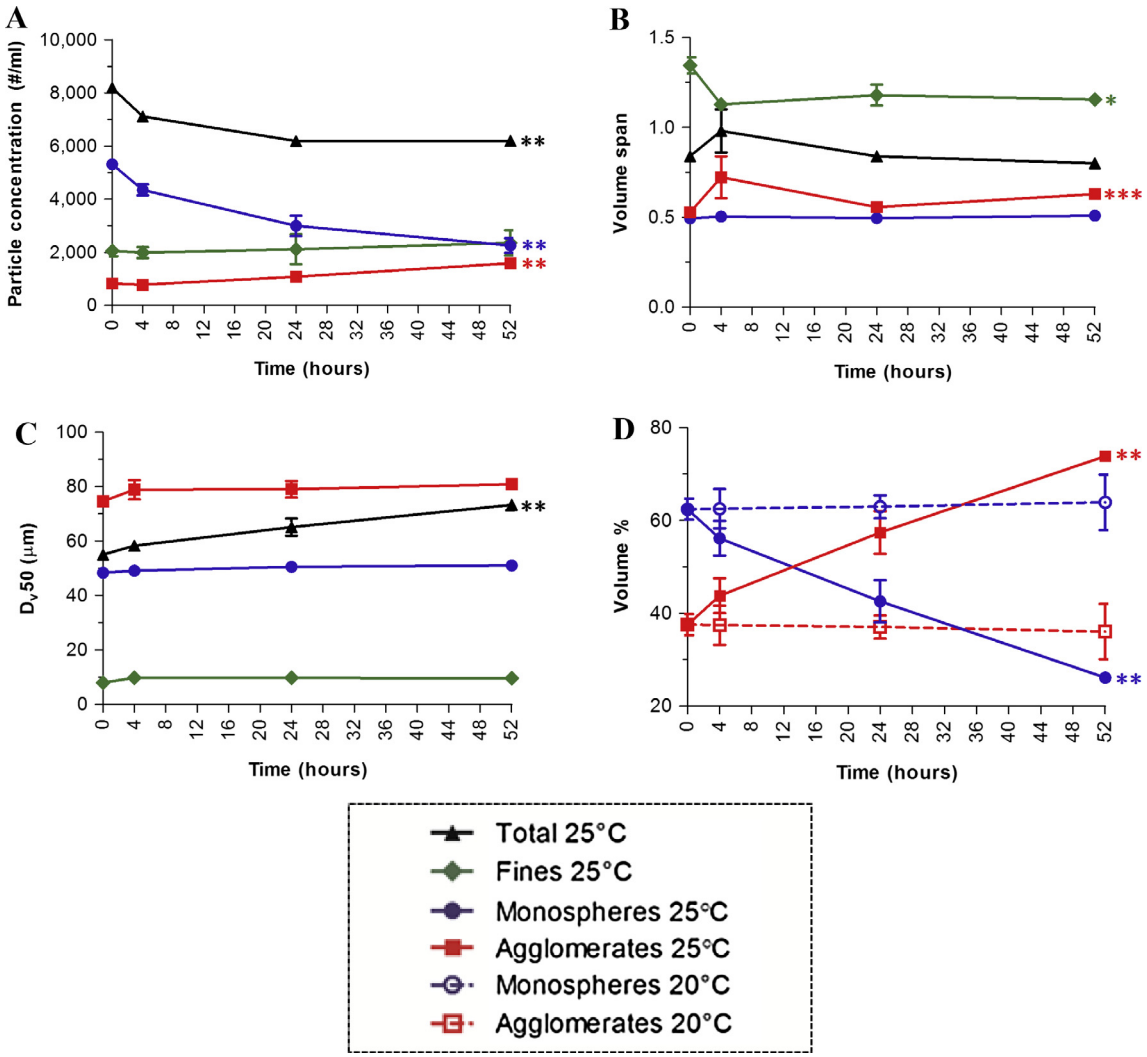

Fig. 9. Stability of Sandostatin LAR monitored with Micro-Flow Imaging and measured at 0, 4, 24 and 52 h after reconstitution. The (A) particle concentration, (B) volume span, and (C) median particle size of the different particle populations (i.e. total, fines, monospheres and agglomerates) in reconstituted Sandostatin LAR incubated at 25 °C are presented. Moreover, the (D) volume percentages of monospheres and agglomerates are shown during incubation at 20 °C (dashed lines) and 25 °C (solid lines). Results are the mean of two samples (±standard deviation). Unpaired, two tailed t tests were performed to compare the results at 0 and 52 h (* $p < 0.05$, ** $p < 0.01$, *** $p < 0.001$).

an increase in the Dv50 of the fines, monospheres or agglomerates (Fig. 9C). However, the Dv50 shift of the total particle population could be explained by a substantial increase in the volume percentage of agglomerates (from 37.5 ± 2.3% at 0 h to 73.9 ± 1.0% at 52 h), together with an equivalent decrease in the volume percentage of monospheres (from 62.4 ± 2.3% at 0 h to 26.1 ± 1.0% at 52 h) (Fig. 9D). Remarkably, there was no significant increase or decrease in the volume percentage of any of the populations for reconstituted Sandostatin LAR incubated at 20 °C for 52 h (Fig. 9D).

The substantial agglomeration propensity of reconstituted Sandostatin LAR at 25 °C may be related to the use of PLGA-glucose star polymer instead of the normal PLGA polymer. In PLGA-glucose star polymer, the free acid end groups of PLGA are reacted with the hydroxyl groups of a core glucose unit, forming a star-shaped structure. PLGA-glucose has several advantages over conventional PLGA for encapsulating proteins and peptides (such as octreotide) [36]. Most importantly, it limits the initial burst release that poses a serious threat in terms of toxicity. It also features longer polymer degradation times and reduced risk of acylation of the encapsulated protein or peptide, owing to the absence of free acid end groups.

Another characteristic of PLGA-glucose microparticles is that hydration is enhanced due to the presence of the hydrophilic glucose core [37–39]. The T_g of PLGA-based products is known to decrease tremendously upon hydration following reconstitution [40,41]. Kang et al. [39] concluded that the polymer chains at the surface of PLGA-glucose microparticles rapidly became more flexible within 2 h of hydration and formed a nonporous film on the previously porous surface. We suggest that in our case study the T_g of the PLGA-glucose polymers on the surface of reconstituted Sandostatin LAR decreased to a temperature close to 25 °C within 4 h of reconstitution. Incubation at 25 °C, but not at 20 °C, may have modified the surface of the reconstituted PLGA-glucose microparticles, resulting in reduced physical and colloidal stability, which led to enhanced agglomeration.

4. Final remarks and conclusions

In this study, we reported the use of MFI (a flow imaging microscope) to characterize PLGA microparticles that serve as drug delivery systems for small molecules or peptides. The size distribution of PLGA microparticles is commonly assessed with a static light scattering or laser diffraction instrument such as Mastersizer. The two techniques, Mastersizer and MFI, are based on different mea-

Table 4
Technical comparison between the Mastersizer 2000 and Micro-Flow Imaging 5100 instruments for the analysis of particle size distribution [15,16,25].

	Mastersizer 2000	MFI 5100
Specifications		
Measurement principle	Laser diffraction according to Fraunhofer or Mie theory	Digital microscopy of sample passing through a flow cell
Sizing range	0.02–2000 μm	2–300 μm
Sample type	Suspension, also dry option	Suspension
Concentration range	Concentration must be adjusted to a light obscuration level of 5–50% (ideally 10–20%)	2.5-μm particles: 0–175,000/ml 5-μm particles: 0–75,000/ml 10-μm particles: 0–20,000/ml
Light source	HeNe laser 633 nm (red), LED 466 nm (blue)	LED light
Detection	Detector array for forward, side and back scattering	High frequency acquisition of microscopic images
Solvent compatibility	Wide range of solvents	Aqueous sample fluids; limited compatibility with organic solvents
Instrument operation		
Level of training	Basic	Basic for acquisition; moderate to high for data processing
Measurement time	One to several minutes per sample, optional autosampler	Several minutes per sample, optional autosampler
Sample consumption	High; e.g., 50–150 mg of PLGA microparticles in suspension	Low; e.g., 0.5–1 mg of PLGA microparticles in suspension
Principle output	Volume-based, equivalent spherical diameter	Number-based, equivalent circular diameter
Sample visualization	No	Yes
Contamination	Air bubbles may be detected by light intensity fluctuations	Morphology can help to differentiate contaminants
Applications		
Sizing	Yes	Yes
Counting	No	Yes
Morphology	No	Yes; aspect ratio, circularity, maximum Feret diameter, transparency of particles
Agglomeration	No; only size shift	Yes; quantitative assessment

surement principles and display unique capabilities for particle size analysis (Table 4).

We showed that Mastersizer and MFI measured similar volume-based size distributions for the total particle population of two commercial PLGA microparticle products (Fig. 2B and D). We also demonstrated two key advantages of MFI over Mastersizer: (1) MFI provides an actual number-based size distribution due to the detection of individual particles (=quantitative method), and (2) MFI enables the classification of PLGA microparticles into distinct particle populations (i.e., fines, monospheres and agglomerates) based on morphological characteristics.

The size, quantity and morphology of particles in these subpopulations are important quality attributes of a PLGA microparticle product. For instance, if the size of the monospheres decreases, this will increase the surface-area-to-volume ratio and thus increase the rate of drug diffusing out of the particles [42]. Also, water will more easily enter smaller particles owing to their larger surface area, resulting in an enhanced "burst release" effect and more rapid hydrolytic degradation of PLGA polymers. On the other hand, an increase in PLGA microparticle size results in a decrease in particle surface area, which will lead to a decrease in drug release rate [43].

One particularly interesting application of MFI in the analysis of PLGA microparticles is that it can determine whether a shift to larger sizes in a product is due to particles growing in size or particle agglomeration. In case of particle growth, one would expect to see a reduction in drug release rate. By contrast, agglomeration of particles would result in accelerated drug release due to the retention of acidic PLGA degradation products inside the agglomerates, which auto-catalyze hydrolysis of the polymers [26,44]. Moreover, the surface area of an agglomerate consisting of multiple microparticles that are fused together is substantially larger than that of one large microparticle with the same diameter as the agglomerate. Lastly, agglomeration not only affects drug release rate but may also compromise suspendability and injectability of a PLGA microparticle product [43].

In conclusion, we have presented MFI as a valuable tool to assess the size and agglomeration of PLGA microparticles, which can serve to promote insight into the relationship between the formulation and process parameters, particle characteristics, physical stability, drug release and (ultimately) the clinical efficacy of these types of products.

Acknowledgments

The authors acknowledge Theo Krikken and Kor Kostwinder for their help with performing MFI and Mastersizer measurements, and Jeroen van Vught for his valuable suggestions and scientific discussion. Wim Jiskoot is scientific advisor at Coriolis Pharma, Martinsried, Germany.

References

[1] S.P. Schwendeman, R.B. Shah, B.A. Bailey, A.S. Schwendeman, Injectable controlled release depots for large molecules, J. Control. Release 190 (2014) 240–253.
[2] D.J. Hines, D.L. Kaplan, Poly(lactic-co-glycolic acid) controlled release systems: experimental and modeling insights, Crit. Rev. Ther. Drug Carrier Syst. 30 (2013) 257–276.
[3] H.K. Makadia, S.J. Siegel, Poly lactic-co-glycolic acid (PLGA) as biodegradable controlled drug delivery carrier, Polymers 3 (2011) 1377–1397.
[4] S.S. D'Souza, J.A. Faraj, P.P. DeLuca, A model-dependent approach to correlate accelerated with real-time release from biodegradable microspheres, AAPS PharmSciTech 6 (2005) E553–E564.
[5] Janssen Pharmaceuticals, Risperdal Consta® (Risperidone) Long-acting Injection – Highlights of Prescribing Information, 2007. <https://www.janssencns.com/shared/product/risperdalconsta/prescribing-information.pdf>.
[6] Novartis, Sandostatin® LAR Depot (Octreotide Acetate for Injectable Suspension) Prescribing Information, 2016. <https://www.pharma.us.novartis.com/sites/www.pharma.us.novartis.com/files/sandostatin_lar.pdf>.
[7] Y. Bahl, H. Sah, Dynamic changes in size distribution of emulsion droplets during ethyl acetate-based microencapsulation process, AAPS PharmSciTech 1 (2000) 41–49.
[8] Z. Su, F. Sun, Y. Shi, C. Jiang, Q. Meng, L. Teng, Y. Li, Effects of formulation parameters on encapsulation efficiency and release behavior of risperidone poly(D,L-lactide-co-glycolide) microsphere, Chem. Pharm. Bull. 57 (2009) 1251–1256.
[9] S. D'Souza, J.A. Faraj, S. Giovagnoli, P.P. DeLuca, Development of risperidone PLGA microspheres, J. Drug Deliv. (2014) 1–11 Article ID 620464.
[10] C. Berkland, K. Kim, D.W. Pack, PLG microsphere size controls drug release rate through several competing factors, Pharm. Res. 20 (2003) 1055–1062.
[11] D. Klose, F. Siepmann, K. Elkharraz, S. Krenzlin, J. Siepmann, How porosity and size affect the drug release mechanisms from PLGA-based microparticles, Int. J. Pharm. 314 (2006) 198–206.

[12] F. Gabor, B. Ertl, M. Wirth, R. Mallinger, Ketoprofen-poly(D,L-lactic-co-glycolic acid) microspheres: influence of manufacturing parameters and type of polymer on the release characteristics, J. Microencapsul. 16 (1999) 1–12.
[13] S. De, D.H. Robinson, Particle size and temperature effect on the physical stability of PLGA nanospheres and microspheres containing Bodipy, AAPS PharmSciTech 5 (2004) 18–24.
[14] D. Klose, F. Siepmann, J.F. Willart, M. Descamps, J. Siepmann, Drug release from PLGA-based microparticles: effects of the "microparticle:bulk fluid" ratio, Int. J. Pharm. 383 (2010) 123–131.
[15] Malvern Instruments, Mastersizer 2000 user manual, in: MAN0384 Issue 1.0, Worcestershire, UK, March 2007.
[16] L.O. Narhi, V. Corvari, D.C. Ripple, N. Afonina, I. Cecchini, M.R. Defelippis, P. Garidel, A. Herre, A.V. Koulov, T. Lubiniecki, H.C. Mahler, P. Mangiagalli, D. Nesta, B. Perez-Ramirez, A. Polozova, M. Rossi, R. Schmidt, R. Simler, S. Singh, T. M. Spitznagel, A. Weiskopf, K. Wuchner, Subvisible (2–100 μm) particle analysis during biotherapeutic drug product development: part 1, considerations and strategy, J. Pharm. Sci. 104 (2015) 1899–1908.
[17] G.A. Wilson, M.C. Manning, Flow imaging: moving toward best practices for subvisible particle quantitation in protein products, J. Pharm. Sci. 102 (2013) 1133–1134.
[18] S. Zölls, D. Weinbuch, M. Wiggenhorn, G. Winter, W. Friess, W. Jiskoot, A. Hawe, Flow imaging microscopy for protein particle analysis – a comparative evaluation of four different analytical instruments, AAPS J. 15 (2013) 1200–1211.
[19] D. Weinbuch, S. Zolls, M. Wiggenhorn, W. Friess, G. Winter, W. Jiskoot, A. Hawe, Micro-flow imaging and resonant mass measurement (Archimedes)–complementary methods to quantitatively differentiate protein particles and silicone oil droplets, J. Pharm. Sci. 102 (2013) 2152–2165.
[20] A.S. Sediq, M.R. Nejadnik, I. El Bialy, G.J. Witkamp, W. Jiskoot, Protein-polyelectrolyte interactions: monitoring particle formation and growth by nanoparticle tracking analysis and flow imaging microscopy, Eur. J. Pharm. Biopharm. 93 (2015) 339–345.
[21] C.J. Farrell, S.M. Cicalese, H.B. Davis, B. Dogdas, T. Shah, T. Culp, V.M. Hoang, Cell confluency analysis on microcarriers by micro-flow imaging, Cytotechnology 68 (2016) 2469–2478.
[22] M. Ramstack, G.P. Grandolfi, E. Mannaert, P. D'Hoore, R.A. Lasser, Long-acting risperidone: prolonged-release injectable delivery of risperidone using Medisorb® microsphere technology, Schizophr. Res. 60 (Suppl. 1) (2003) 314.
[23] S.E. Grady, S.V. Andurkar, Psychiatric disorders and substance-related disorders, in: A. Desai, M. Lee (Eds.), Gibaldi's Drug Delivery Systems in Pharmaceutical Care, American Society of Health-System Pharmacists, Bethesda, Maryland, 2007 (Chapter 17).
[24] H. Petersen, J.-C. Bizec, H. Schuetz, M.-L. Delporte, Pharmacokinetic and technical comparison of Sandostatin® LAR® and other formulations of long-acting octreotide, BMC Res. Notes 4 (2011) 1–8.
[25] ProteinSimple, User manual MFI view analysis suite release 1.3, in: Document D-0000052-00_04, ProteinSimple, Ottawa, Ontario, Canada, October 2011.
[26] C. Wischke, S.P. Schwendeman, Principles of encapsulating hydrophobic drugs in PLA/PLGA microparticles, Int. J. Pharm. 364 (2008) 298–327.
[27] A. Mahboubian, S.K. Hashemein, S. Moghadam, F. Atyabi, R. Dinarvand, Preparation and in-vitro evaluation of controlled release PLGA microparticles containing triptoreline, Iran. J. Pharm. Res. 9 (2010) 369–378.
[28] N. Kiss, G. Brenn, D. Suzzi, S. Scheler, H. Jennewein, J. Wieser, J. Khinast, The influence of process parameters on the properties of PLGA-microparticles produced by the emulsion extraction method, AIChE J. 59 (2013) 1868–1881.
[29] S. Puthli, P. Vavia, Formulation and performance characterization of radio-sterilized "progestin-only" microparticles intended for contraception, AAPS PharmSciTech 10 (2009) 443–452.
[30] Y.-Y. Yang, T.-S. Chung, X.-L. Bai, W.-K. Chan, Effect of preparation conditions on morphology and release profiles of biodegradable polymeric microspheres containing protein fabricated by double-emulsion method, Chem. Eng. Sci. 55 (2000) 2223–2236.
[31] H. Sah, Microencapsulation techniques using ethyl acetate as a dispersed solvent: effects of its extraction rate on the characteristics of PLGA microspheres, J. Control. Release 47 (1997) 233–245.
[32] H. Sah, Ethyl formate – alternative dispersed solvent useful in preparing PLGA microspheres, Int. J. Pharm. 195 (2000) 103–113.
[33] A.S. Zidan, Z. Rahman, M.A. Khan, Online monitoring of PLGA microparticles formation using Lasentec focused beam reflectance (FBRM) and particle video microscope (PVM), AAPS J. 12 (2010) 254–262.
[34] A. Cabana, R.B. De, P. Markland, Microspheres for Sustained Release of Octreotide Acetate, Google Patents, 2011. <https://www.google.com/patents/WO2011112576A1?cl=en>.
[35] G. Gill-Sangha, NDA-21346 Chemistry Review(s) Risperdal Consta, Johnson & Johnson Pharmaceutical Research, U.S. Food and Drug Administration, 2003. <http://www.accessdata.fda.gov/drugsatfda_docs/nda/2003/21346_RisperdalTOC.cfm>.
[36] R.H. Ansary, M.M. Rahman, M.B. Awang, H. Katas, H. Hadi, F. Mohamed, A.A. Doolaanea, Y.B. Kamaruzzaman, Preparation, characterization and in vitro release study of BSA-loaded double-walled glucose-poly(lactide-co-glycolide) microspheres, Arch. Pharm. Res. 1–15 (2016).
[37] Y. Yamaguchi, M. Takenaga, A. Kitagawa, Y. Ogawa, Y. Mizushima, R. Igarashi, Insulin-loaded biodegradable PLGA microcapsules: initial burst release controlled by hydrophilic additives, J. Control. Release 81 (2002) 235–249.
[38] J. Wang, B.M. Wang, S.P. Schwendeman, Mechanistic evaluation of the glucose-induced reduction in initial burst release of octreotide acetate from poly(D,L-lactide-co-glycolide) microspheres, Biomaterials 25 (2004) 1919–1927.
[39] J. Kang, S.P. Schwendeman, Pore closing and opening in biodegradable polymers and their effect on the controlled release of proteins, Mol. Pharm. 4 (2007) 104–118.
[40] S.S. Shah, Y. Cha, C.G. Pitt, Poly(glycolic acid-co-DL-lactic acid): diffusion or degradation controlled drug delivery?, J Control. Release 18 (1992) 261–270.
[41] N. Passerini, D.Q.M. Craig, An investigation into the effects of residual water on the glass transition temperature of polylactide microspheres using modulated temperature DSC, J. Control. Release 73 (2001) 111–115.
[42] D.S. Kohane, Microparticles and nanoparticles for drug delivery, Biotechnol. Bioeng. 96 (2007) 203–209.
[43] M.B. DeYoung, L. MacConell, V. Sarin, M. Trautmann, P. Herbert, Encapsulation of exenatide in poly-(D,L-lactide-co-glycolide) microspheres produced an investigational long-acting once-weekly formulation for type 2 diabetes, Diab. Technol. Ther. 13 (2011) 1145–1154.
[44] P. Sansdrap, A.J. Moës, In vitro evaluation of the hydrolytic degradation of dispersed and aggregated poly(DL-lactide-co-glycolide) microspheres, J. Control. Release 43 (1997) 47–58.